Solid-State Chemistry-Enabled Scalable Production of Octahedral Pt-Ni Alloy Electrocatalyst for Oxygen Reduction Reaction

ARTICLE *in* JOURNAL OF THE AMERICAN CHEMICAL SOCIETY · MAY 2014

Impact Factor: 12.11 · DOI: 10.1021/ja501293x · Source: PubMed

4 AUTHORS, INCLUDING:

Changlin Zhang
University of Akron
10 PUBLICATIONS **53** CITATIONS

SEE PROFILE

JACS
JOURNAL OF THE AMERICAN CHEMICAL SOCIETY
Communication
pubs.acs.org/JACS

Solid-State Chemistry-Enabled Scalable Production of Octahedral Pt–Ni Alloy Electrocatalyst for Oxygen Reduction Reaction

Changlin Zhang, Sang Youp Hwang, Alexis Trout, and Zhenmeng Peng*

Department of Chemical and Biomolecular Engineering, University of Akron, Akron, Ohio 44325, United States

Supporting Information

ABSTRACT: Although octahedral Pt–Ni alloy nanoparticles possess an excelling property in oxygen reduction reaction (ORR) and are of great potential as an electrocatalyst for polymer electrolyte membrane fuel cells (PEMFCs), mass production of the materials at low cost remains a big challenge. By combining the advantages of both solid-state chemistry and wet synthetic chemistry, we developed one scalable, surfactant-free, and cost-effective method for producing octahedral Pt–Ni alloy nanoparticles on carbon support. The octahedral Pt–Ni samples were prepared with different compositions and studied for the ORR property. They exhibit a much improved reaction activity compared to the commercial catalyst. The experiments demonstrate an innovative strategy for preparing shaped metal nanoparticles and make significant progress in the ORR catalyst research.

The commercial viability of the polymer electrolyte membrane fuel cell (PEMFC) technology, despite its great promise in both energy efficiency and environmental control, has been hindered by the development of oxygen reduction reaction (ORR) catalysts.[1−4] Large amounts of precious Pt metal is required to promote the sluggish kinetics, causing the PEMFCs to be economically uncompetitive with conventional technologies. To advance the technology, the Pt usage must be significantly reduced, with targets of 0.7 mA/cm^2 Pt and 0.44 A/mg Pt at 0.9 V for active area and mass-specific ORR activities set by the DOE.[5] Intensive research activities have been conducted in search of active Pt structures in the past years to reach the targets, which led to the development of many types of alloy,[6−12] skin-layer,[13−16] core–shell, and thin-film electrocatalysts.[17−20]

The recent discovery that Pt_3Ni (111) crystal surface can exhibit an exceptionally high ORR activity of 18 mA/cm^2 Pt has motivated the preparation of octahedral Pt–Ni alloy nanoparticles, which are enclosed by the (111) planes and have a large specific active area.[6] Several research groups have made good progress by synthesizing octahedral Pt–Ni particles and reporting high ORR activity, which demonstrates that the strategy is very promising to solve the catalyst problems.[7,21−24] However, the wet synthetic methods developed in these experiments have low scaling-up capacity and are thus not suitable for mass production of the octahedral Pt–Ni catalyst. Moreover, organic surfactants are usually employed to control the particle morphology, which contaminate the surface and require careful cleanings before the particles become catalytically active.[25] The complex contaminants removal and synthetic procedures add much production cost and make these techniques economically unfeasible. In this regard, a new method for mass production of the octahedral Pt–Ni alloy electrocatalyst is highly desirable.

Here we report a scalable, surfactant-free, and low-cost solid-state chemistry method for mass production of octahedral Pt–Ni alloy nanoparticles on carbon support (Pt–Ni/C) and demonstrate high ORR activity of the made catalyst. Octahedral Pt–Ni/C was prepared by simply impregnating both metal acetylacetonates onto a C support and reducing them at 200 °C in 120/5 cm^3/min CO/H_2 for 1 h (see Supporting Information for more details). A batch preparation of 2 g octahedral $Pt_{1.5}Ni$/C (20 wt % Pt) is demonstrated using the innovative method (Figure 1A), which can be facilely scaled up for mass production of the materials. Little influence on the octahedral morphology of the $Pt_{1.5}Ni$ particles is observed when the Pt loading is varied between 10 and 40 wt %, indicating robustness of the method (Figure S1).

X-ray diffraction (XRD) of the product exhibits peaks that belong to (111), (200), and (220) planes of a face-centered cubic (fcc) lattice (Figure S2). The fact that there are no other diffraction peaks and that the observed ones fall in between those for pure Pt and Ni metals suggests the formation of uniform Pt–Ni alloy. Most of the particles are seen in a rhombic shape with straight edges, with an average edge length of 5.8 ± 1.5 nm (Figure 1B). The observations suggest the solid-state chemistry method is effective in making uniform $Pt_{1.5}Ni$ alloy particles and meanwhile controlling their morphology. Quantitative analysis of the product using energy dispersive X-ray (EDX) spectroscopy determines a Pt/Ni molar ratio of 1.45 (Figure 1C), which is very close to the amount of metal precursors being used. The lattice fringes have a measured inner-planar distance of 2.13 Å and can be indexed to the (111) planes (Figure 1D). The value is significantly smaller than 2.27 Å for the fcc Pt (111), which provides additional evidence for the formation of Pt–Ni alloy. The observation that the rhombic edges are parallel to these lattice fringes reveals that the $Pt_{1.5}Ni$ particles are enclosed by the (111) surfaces and have an octahedral morphology. Figure 1E–G shows high-angle annular dark-field scanning TEM (HAADF-STEM) of one individual octahedral $Pt_{1.5}Ni$ particle and corresponding EDX maps for the two elements. Both metals are distributed throughout the entire particle and have a

Received: February 11, 2014
Published: May 14, 2014

   dx.doi.org/10.1021/ja501293x | J. Am. Chem. Soc. 2014, 136, 7805−7808

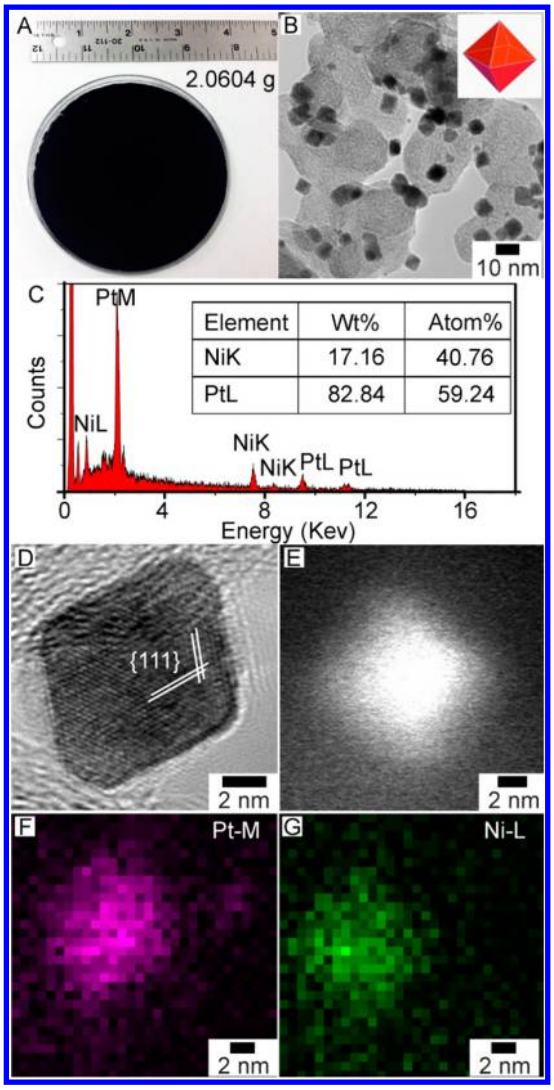

Figure 1. Characterization of octahedral $Pt_{1.5}Ni$/C. (A) Gram-scale production. (B, C) TEM image and EDX profile of octahedral $Pt_{1.5}Ni$/C sample, and (D) HRTEM, (E) HAADF-STEM, and (F, G) EDX elemental mapping of one individual particle.

similar size to the STEM image, indicating a uniform alloy composition.

The solid-state chemistry method is effective in preparing octahedral Pt−Ni/C within composition range from Pt_4Ni to PtNi, whereas truncated octahedrons and cubes are produced with a less amount of Ni precursor (Figure S3). The composition-dependent morphology change could be associated with CO adsorption to the two metals. Both experimental and theoretical studies suggest that CO molecules adsorb preferentially to (100) planes for Pt but to (111) for Ni,[26,27] which can alter the growth rate of surface planes and therefore the resultant particle morphology. Thus, Pt−Ni tends to grow into octahedrons when Ni content is sufficiently high to dominate the CO adsorption, and pure Pt tends to grow into cubes, with truncated shape resulting in between. Figure S4 shows the Fourier transform infrared (FTIR) spectrum of freshly made octahedral $Pt_{1.5}Ni$ nanoparticles, which exhibited an intensive CO absorbance band before the sample was exposed to air. The band, centered at around 2071 cm^{-1} and assignable to linearly bonded CO,[28] confirms strong adsorption of the molecules to the Pt−Ni (111) surface. The absorbance peak diminished rapidly after exposure of the sample to air, which indicates an efficient CO removal and thus clean particles surface after synthesis. The removal of adsorbed CO is likely caused by CO oxidation, because Pt−Ni can actively catalyze the reaction even at room temperature.[29]

H_2 is employed for facilitating transportation of both metal precursors on the C support and reducing them into alloys.[28,30,31] The Pt−Ni particles prepared with pure CO, 3.1 ± 1.2 nm in size and a mixture of octahedron and polyhedron in morphology, are significantly smaller than those prepared in CO/H_2 (Figures S5−S6). The alloy particles prepared with pure H_2, on the other side, are spherical and dramatically bigger in size. The loss of octahedral morphology in pure H_2 confirms that CO is responsible for making shaped Pt−Ni, and the formation of small polyhedral particles in CO could result from a limited supply of metal precursors to the growing sites due to their insufficient transportation. The formation of perfect octahedral particles seems to favor a high CO partial pressure, with truncated octahedrons being produced when H_2 partial pressure is high. It could be caused by the competition of H_2 adsorption to Pt−Ni against CO adsorption, which leads to a lower CO coverage on growing particles and thus less control on the shape formation.[30,31]

The Pt−Ni/C samples were collected after different times of reduction at 200 °C in 120/5 cm^3/min CO/H_2 and characterized for studying the growth process of the particles (Figure S7). Octahedral particles with an average length of 3.9 ± 1.0 nm were obtained after 1 min of reaction, suggesting rapid reduction kinetics. They further grew into 4.7 ± 1.2, 5.0 ± 1.1, and 6.0 ± 1.0 nm particles after 5, 30, and 120 min of reaction. The particles obtained at 120 min are of comparable size to those obtained at 60 min, implying completion of the reduction process within 60 min. In comparison, most of the obtained particles are <3 nm after 1 min of reduction when there is only Pt precursor on the support and the Ni precursor by itself cannot be effectively reduced under the specific condition (Figures S8 and S9). The observations suggest that the Pt and Ni precursors could catalyze each other for their reduction. Based on the experimental findings, the growth of octahedral Pt−Ni/C can be schematically illustrated in Scheme 1, wherein H_2 facilitates the transportation of both metal

Scheme 1. Schematic Illustration of the formation of Octahedral Pt−Ni Nanoparticles on C Support under the Synthetic Condition

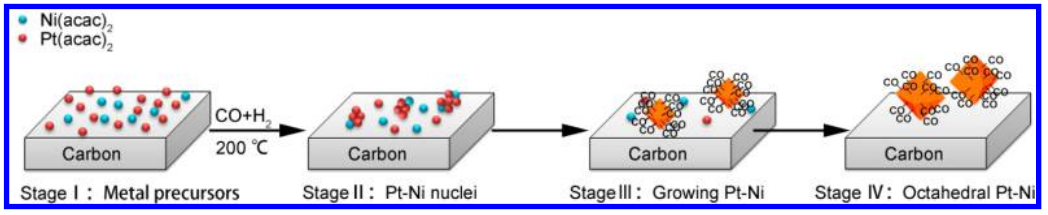

dx.doi.org/10.1021/ja501293x | J. Am. Chem. Soc. 2014, 136, 7805−7808

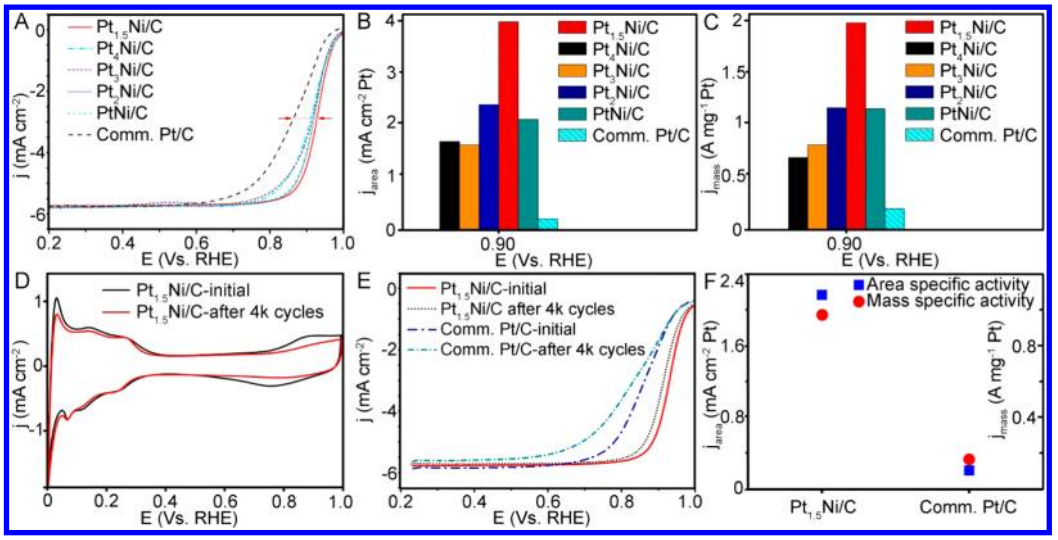

Figure 2. ORR property of octahedral Pt−Ni/C. (A) ORR polarization curves, (B, C) Active area and mass-specified ORR current densities (j_{area} and j_{mass}) of PtNi/C, $Pt_{1.5}Ni/C$, Pt_2Ni/C, Pt_3Ni/C, Pt_4Ni/C, and commercial Pt/C in O_2-saturated 0.1 M $HClO_4$ at room temperature with a scan rate of 10 mV/s and an electrode rotating rate of 1600 rpm. (D) Cyclic voltammograms, (E) ORR, and (F) j_{area} and j_{mass} of $Pt_{1.5}Ni/C$ and commercial Pt/C after accelerated stability tests.

precursors to their growing sites and reduces them into alloys, and CO shapes the growing particles into octahedrons by preferentially adsorbing to the (111) surface planes.

The prepared octahedral PtNi/C, $Pt_{1.5}Ni/C$, Pt_2Ni/C, Pt_3Ni/C, and Pt_4Ni/C samples (containing 20 wt % Pt) were studied for the ORR property. All five catalysts exhibit significantly different features in the hydrogen adsorption−desorption region (HAD, ~0.05 < E < 0.4 V vs RHE) when being compared with commercial Pt/C (Figures S10−S11), which is resultant of variant exposed surface planes.[32] The measured electrochemical active surface areas (ECSAs) based on hydrogen adsorption signals are 54.1, 48.3, 48.1, 49.3, and 40.2 m^2/g Pt for the five catalysts. The decent agreement between the ECSA values and the specific surface areas calculated using the average particle sizes suggests the octahedral Pt−Ni has a clean surface and is electrochemically active without any pretreatment (Table S1).

The ORR activities of the catalysts were measured by collecting the polarization curves and calculating the kinetic current densities using the Koutechy−Levich equation (Figure 2).[33] Comparing to the commercial Pt/C, the half-wave potential for the octahedral $Pt_{1.5}Ni/C$ has a significant shift of 64 mV toward the positive direction, implying much improved reaction kinetics. For quantitative comparisons, the ORR activities were normalized by both the ECSA and the Pt mass. Figure 2B shows the active area-specified ORR kinetic current densities (j_{area}), which represent intrinsic activity of the catalysts. All the five octahedral Pt−Ni/C samples exhibit significantly higher values than the commercial Pt/C, indicating much improved ORR kinetics. The highest j_{area} value appeared with the octahedral $Pt_{1.5}Ni/C$ among the five octahedral Pt−Ni/C samples, suggesting $Pt_{1.5}Ni$ has the most optimal composition for catalyzing the ORR reaction. The finding is consistent with previous studies using octahedral Pt−Ni nanoparticles,[21] in which $Pt_{1.5}Ni$ has also been reported as the best ORR catalyst, although the study using single Pt−Ni crystals suggests an optimal Pt_3Ni composition.[6] The discrepancy between nanoscale and bulk studies could be caused by the different sample dimensions, which can influence electronic structure of the surface. The octahedral $Pt_{1.5}Ni$ nanoparticles, rather than Pt_3Ni, might have the optimal electronic structure for ORR and thus exhibit the highest activity. The octahedral $Pt_{1.5}Ni/C$ exhibits 19.31 and 3.99 mA/cm^2 Pt at 0.85 and 0.90 V vs RHE, which are about 32 and 20 times the values for commercial Pt/C specifically (Figures 2B and S12). The mass-specified kinetic current densities (j_{mass}), which are of more concern for real applications, are 9.47 and 1.96 A/mg Pt at the two potentials for the octahedral $Pt_{1.5}Ni/C$ (Figures 2C and S12). The values are 16 and 10 times as high compared to commercial Pt/C and are among the highest compared to the previous studies on octahedral Pt−Ni nanoparticles.[7,21−24]

The long-term performance of the octahedral $Pt_{1.5}Ni/C$ catalyst was evaluated by conducting an accelerated stability test and comparing the results with the commercial Pt/C. After 4000 cycles of linear potential sweeps between 0.60 and 1.00 V vs RHE at a scan rate of 50 mV/s, the ECSA of the $Pt_{1.5}Ni/C$ decayed by only 8% (Figure 2D). In comparison, the commercial Pt/C had about a 24% loss in the ECSA. The after-test j_{area} and j_{mass} for the $Pt_{1.5}Ni/C$ decreased to 2.17 mA/cm^2 Pt and 0.97 A/mg Pt at 0.9 V vs RHE (Figure 2E,F), which were more than one order and six times of those for the tested Pt/C (0.206 mA/cm^2 Pt and 0.162 A/mg Pt) and still far exceeded the DOE targets.[5] The promising stability of the $Pt_{1.5}Ni/C$ could be associated with the fact that a large portion of the particles largely maintained an octahedral morphology during the stability test (Figure S13). The stability of the octahedral $Pt_{1.5}Ni/C$ can potentially be further improved by optimizing the particle size and the pretreatment condition of the materials, as suggested in recent studies.[7,21,34]

In summary, we realize scalable production of octahedral Pt−Ni/C alloy nanocrystals by innovating a robust, green, and low-cost solid-state chemistry approach. The experiments suggest that the octahedral Pt−Ni production is resultant of employing both CO and H_2 gases, wherein H_2 aids transportation and reduction of the metal precursors on C support and CO is responsible for the particle morphology formation. ORR tests show much improved activity (3.99 mA/cm^2 Pt and 1.96 A/mg Pt at 0.9 V vs RHE) compared to the commercial Pt/C. These results bridge fundamental catalysis studies on Pt−Ni with

dx.doi.org/10.1021/ja501293x | J. Am. Chem. Soc. 2014, 136, 7805−7808

possibilities for real application of the materials to advance the fuel cell technology.

■ ASSOCIATED CONTENT

Supporting Information

Experimental details and characterization procedures, TEM, XRD, CV, and electrochemical data. This material is available free of charge via the Internet at http://pubs.acs.org.

■ AUTHOR INFORMATION

Corresponding Author

zpeng@uakron.edu

Notes

The authors declare no competing financial interest.

■ ACKNOWLEDGMENTS

Supported by the University of Akron start-up fund (Z.P.). TEM data were obtained at the (cryo)TEM facility at the Liquid Crystal Institute, Kent State University, supported by the Ohio Research Scholars Program Research Cluster on Surfaces in Advanced Materials. The authors thank Dr. Min Gao for technical support with the TEM experiments.

■ REFERENCES

(1) Debe, M. K. *Nature* **2012**, *486*, 43.
(2) GreeleyJ; Stephens, I. E. L.; Bondarenko, A. S.; Johansson, T. P.; Hansen, H. A.; Jaramillo, T. F.; RossmeislJ; ChorkendorffI; Nørskov, J. K. *Nat. Chem.* **2009**, *1*, 552.
(3) Gasteiger, H. A.; Marković, N. M. *Science* **2009**, *324*, 48.
(4) Gasteiger, H. A.; Kocha, S. S.; Sompalli, B.; Wagner, F. T. *Appl. Catal., B* **2005**, *56*, 9.
(5) Papageorgopoulos, D. U. S. Deparment of Energy. *Annual Merit Review – Fuel Cells*, May 14, 2012; http://www.hydrogen.energy.gov/pdfs/review12/fc_plenary_papageorgopoulos_2012_o.pdf.
(6) Stamenkovic, V. R.; Fowler, B.; Mun, B. S.; Wang, G.; Ross, P. N.; Lucas, C. A.; Marković, N. M. *Science* **2007**, *315*, 493.
(7) Carpenter, M. K.; Moylan, T. E.; Kukreja, R. S.; Atwan, M. H.; Tessema, M. M. *J. Am. Chem. Soc.* **2012**, *134*, 8535.
(8) Lim, B.; Jiang, M.; Camargo, P. H. C.; Cho, E. C.; Tao, J.; Lu, X.; Zhu, Y.; Xia, Y. *Science* **2009**, *324*, 1302.
(9) Wang, D.; Xin, H. L.; Hovden, R.; Wang, H.; Yu, Y.; Muller, D. A.; DiSalvo, F. J.; Abruña, H. D. *Nat. Mater.* **2013**, *12*, 81.
(10) Wu, J.; Qi, L.; You, H.; Gross, A.; Li, J.; Yang, H. *J. Am. Chem. Soc.* **2012**, *134*, 11880.
(11) Hong, J. W.; Kang, S. W.; Choi, B.-S.; Kim, D.; Lee, S. B.; Han, S. W. *ACS Nano* **2012**, *6*, 2410.
(12) Stephens, I. E. L.; Bondarenko, A. S.; Perez-Alonso, F. J.; Calle-Vallejo, F.; Bech, L.; Johansson, T. P.; Jepsen, A. K.; Frydendal, R.; Knudsen, B. P.; Rossmeisl, J.; Chorkendorff, I. *J. Am. Chem. Soc.* **2011**, *133*, 5485.
(13) Wang, J. X.; Inada, H.; Wu, L.; Zhu, Y.; Choi, Y.; Liu, P.; Zhou, W.-P.; Adzic, R. R. *J. Am. Chem. Soc.* **2009**, *131*, 17298.
(14) Zhang, J.; Lima, F. H. B.; Shao, M. H.; Sasaki, K.; Wang, J. X.; Hanson, J.; Adzic, R. R. *J. Phys. Chem. B* **2005**, *109*, 22701.
(15) Zhang, Y.; Hsieh, Y.-C.; Volkov, V.; Su, D.; An, W.; Si, R.; Zhu, Y.; Liu, P.; Wang, J. X.; Adzic, R. R. *ACS Catal.* **2014**, *4*, 738.
(16) Shao, M.; Shoemaker, K.; Peles, A.; Kaneko, K.; Protsailo, L. *J. Am. Chem. Soc.* **2010**, *132*, 9253.
(17) Zhang, L.; Iyyamperumal, R.; Yancey, D. F.; Crooks, R. M.; Henkelman, G. *ACS Nano* **2013**, *7*, 9168.
(18) Kibsgaard, J.; Gorlin, Y.; Chen, Z.; Jaramillo, T. F. *J. Am. Chem. Soc.* **2012**, *134*, 7758.
(19) Strasser, P.; Koh, S.; Anniyev, T.; Greeley, J.; More, K.; Yu, C.; Liu, Z.; Kaya, S.; Nordlund, D.; Ogasawara, H.; Toney, M. F.; Nilsson, A. *Nat. Chem.* **2010**, *2*, 454.
(20) Debe, M. K.; Schmoeckel, A. K.; Vernstrom, G. D.; Atanasoski, R. *J. Power Sources* **2006**, *161*, 1002.
(21) Cui, C.; Gan, L.; Heggen, M.; Rudi, S.; Strasser, P. *Nat. Mater.* **2013**, *12*, 765.
(22) Choi, S.-I.; Xie, S.; Shao, M.; Odell, J. H.; Lu, N.; Peng, H.-C.; Protsailo, L.; Guerrero, S.; Park, J.; Xia, X.; Wang, J.; Kim, M. J.; Xia, Y. *Nano Lett.* **2013**, *13*, 3420.
(23) Zhang, J.; Yang, H.; Fang, J.; Zou, S. *Nano Lett.* **2010**, *10*, 638.
(24) Wu, J.; Zhang, J.; Peng, Z.; Yang, S.; Wagner, F. T.; Yang, H. *J. Am. Chem. Soc.* **2010**, *132*, 4984.
(25) Niu, Z.; Li, Y. *Chem. Mater.* **2013**, *26*, 72.
(26) Morikawa, Y.; Mortensen, J. J.; Hammer, B.; Nørskov, J. K. *Surf. Sci.* **1997**, *386*, 67.
(27) Palaikis, L.; Zurawski, D.; Hourani, M.; Wieckowski, A. *Surf. Sci.* **1988**, *199*, 183.
(28) Peng, Z.; Kisielowski, C.; Bell, A. T. *Chem. Commun.* **2012**, *48*, 1854.
(29) Ko, E.; Park, E. D.; Seo, K. W.; Lee, H. C.; Lee, D.; Kim, S. *Catal. Lett.* **2006**, *110*, 275.
(30) Zhang, C.; Hwang, S. Y.; Peng, Z. *J. Mater. Chem. A* **2013**, *1*, 14402.
(31) Womes, M.; Cholley, T.; Peltier, F. L.; Morin, S.; Didillon, B.; Szydlowski-Schildknecht, N. *Appl. Catal., A* **2005**, *283*, 9.
(32) Yeager, E.; O'Grady, W. E.; Woo, M. Y. C.; Hagans, P. *J. Electrochem. Soc.* **1978**, *125*, 348.
(33) Wang, S.; Yu, D.; Dai, L. *J. Am. Chem. Soc.* **2011**, *133*, 5182.
(34) Kang, S. W.; Lee, Y. W.; Kim, M.; Hong, J. W.; Han, S. W. *Chem.—Asian J.* **2011**, *6*, 909.